HHS Public Access

Author manuscript

Curr Eye Res. Author manuscript; available in PMC 2018 May 01.

Published in final edited form as:

Curr Eye Res. 2017 May ; 42(5): 721–731. doi:10.1080/02713683.2016.1231325.

Changes in the properties and organization of human lens lipid membranes occurring with age

Laxman Mainali[a], **Marija Raguz**[b], **William J. O'Brien**[c], and **Witold K. Subczynski**[a,*]

[a]Department of Biophysics, Medical College of Wisconsin, Milwaukee, WI 53226, USA

[b]Department of Medical Physics and Biophysics, School of Medicine, University of Split, Split, Croatia

[c]Department of Ophthalmology, Medical College of Wisconsin, Milwaukee, WI 53226, USA

Abstract

Purpose—This research was undertaken to document the changes in the organization and properties of human lens lipid membranes that occur with age.

Materials and Methods—Human lens lipid membranes prepared from the total lipids extracted from clear lens cortices and nuclei of donors from age groups 0–20 and 21–40 years were investigated. An electron paramagnetic resonance technique and nitroxide spin labels (analogues of phospholipids and cholesterol) were used.

Results—Two distinct lipid domains, the phospholipid-cholesterol domain (PCD) and the pure cholesterol bilayer domain (CBD), were detected in all investigated membranes. Profiles of the acyl chain order, fluidity, hydrophobicity, and oxygen transport parameter across discriminated coexisting lipid domains were assessed. Independent of the age-related changes in phospholipid composition, the physical properties of the PCD remained the same for all age groups and were practically identical for cortical and nuclear membranes. However, the properties of pure CBDs changed significantly with the age of the donor and were related to the size of the CBD, which increased with the age of the donor and was greater in nuclear than in cortical membranes. A more-detailed analysis revealed that the size of the CBD was determined mainly by the cholesterol content in the membrane.

Conclusions—This paper presents data from four age groups: 0–20, 21–40, 41–60, and 61–70 years. Data from age groups 41–60 and 61–70 years were published previously. Combining the previously published data with those data obtained in the present work allowed us to show the changes in the organization of cortical and nuclear lens lipid membranes as functions of age and cholesterol. It seems that the balance between age-related changes in membrane phospholipid composition and cholesterol content plays an integral role in the regulation of cholesterol-dependent processes in fiber cell membranes and in the maintenance of fiber cell membrane homeostasis.

*Corresponding Author: Witold K. Subczynski, Department of Biophysics, Medical College of Wisconsin, 8701 Watertown Plank Road, Milwaukee, WI 53226, USA, Tel: (414) 955-4038; Fax: (414) 955-6512; subczyn@mcw.edu.

Declaration of Interest

The authors report no conflicts of interest.

Keywords

cholesterol; cholesterol bilayer domain; cholesterol crystals; membrane domains; spin labeling

Introduction

Our research focuses on the role of the fiber cell plasma membrane in maintaining lens transparency. The plasma membrane together with the cytoskeleton are the only supramolecular structures of the mature fiber cells[1–3] and most of fiber-cell lipids are present in the plasma membrane. In adult lenses, two-thirds of phospholipids (PLs) are sphingolipids, mainly dihydrosphingolipids.[4] The composition changes with age,[5–8] with the additional increase of sphingolipid content and depletion of phosphatidylcholine.[4,7,9,10] Also, the saturation level of PL acyl chains is very high and increases with age.[4,7,11] The cholesterol (Chol) content is the extremely high, reaching a value up to the Chol/PL molar ratio of 4 in aged lenses.[11–14] At such a high level, Chol saturates the PL bilayer, and forms the pure CBDs[15,16] and Chol crystals (presumably outside the fiber cell membranes).[17,18] It is unclear what mechanisms regulate the Chol content of the lens, and it is unknown if the appearance of CBDs, and/or Chol crystals, is harmful or beneficial for lens function.[15,17,19] Chol-lowering drugs increase the risk of developing cataracts; thus, it can be hypothesized that the high Chol content of the lens is beneficial.[20–23] The Chol content of the lens from the older population is often high enough to induce the formation of Chol crystals.[17,18] Minute Chol crystals found in arterial cells can initiate and promote atherosclerosis by activating inflammasomes[24] and inflamation. However, inflammation does not appear to play a role in cataract formation. Are these crystals harmful for the lens? It seems that Chol crystals are not harmful in the lens. Based on our studies, we have concluded that high Chol content, formation of CBDs, and formation of Chol crystals should not be considered major predispositions for the development of age-related cataracts.[8]

Studies on model membranes indicate that the addition of Chol markedly decreased the binding of α-crystallin to liposomes made of sphingomyelin or saturated phosphatidylcholine.[25] The association of α-crystallin with the membrane is accompanied by increased light scattering. The Chol contents used in these experiments were high enough to induce the formation of CBDs, which suggests that high Chol and formation of CBDs can prevent cataract development. It is likely, however, that in intact membranes, this beneficial effect of Chol on light scattering is compensated by the effect of integral membrane proteins. It was shown that during aging, and in the case of cataract formation, the association of α-crystallin with the membrane and light scattering increase.[26–28]

The studies reported here focus on the functions of the lipid bilayer portion of lens fiber cell plasma membranes in the absence of membrane proteins.[29,30] We found that intact membranes lipids are distributed between three distinct lipid environments: bulk lipid domain, which appears minimally affected by membrane proteins, and two domains that appear due to the presence of membrane proteins, namely boundary and trapped lipid domains.[7] The CBD in intact membranes, which was clearly detected in human lens lipid membranes for all age groups, was not detected, possibly because the oxygen transport

parameter measured in the CBD is the same as in the domain formed by trapped lipids. We were able to document age-related changes in the amounts of PLs and Chol in these domains.[6] The amount of boundary and trapped PLs is greater in nuclear than in cortical membranes and increases with the age. The same is true for Chol in trapped lipid domains. Interestingly, Chol was substantially excluded from the trapped lipid domain in cortical membranes. Age-related changes in the organization of lipids correlate well with the changes in the amount and the organization of lens membrane proteins. Aged fiber-cell membranes are loaded with integral proteins,[1,31,32] the organization of which—including the formation of domains, arrays, and other structures—also changes with age.[33–39] It has been shown[34] that the ordered arrays of aquaporin-0 are enriched in the nucleus. This finding is consistent with our current data,[40] which show that the amount of trapped lipid and the extent of lipid rigidity are greater in the nucleus than in the cortex. We can conclude that both the amount of protein and the packing of protein in membranes from the nucleus might be important in modifying the observed lipid physical properties. Also, it is suggested that, in addition to channel functions, fiber cell membranes have specialized aquaporin-0-lipid interactions that determine the cell shape, surface topology, intercellular junctions, and important features of membrane aging and cataract formation[41]. To assess the contributions of integral proteins into the properties and organization of the lipid bilayer portion in intact fiber cells, first, the organization and the properties of membranes prepared from the total lipids extracted from these membranes must be clearly understood. Our previous studies of human lens lipid membranes examined only membranes isolated from the cortices and nuclei of donors aged 41 years and older.[18,42] Combining the previously published data with those data obtained here for age groups 0–20 and 21–40 years presents the broad picture of the changes in the organization of cortical and nuclear lens lipid membranes as functions of age and Chol content.

The major conclusions from the presented work can be summarized as follows: The organization and properties of lens lipid membranes, both in the lens cortex and nucleus, are not determined by the PL composition, which changes drastically with the age of the donor.[5–9,12,13,43] Rather, changes are defined by the Chol content in these membranes. In all age groups, the content of Chol was high enough to saturate the PL bilayer and form pure CBDs. We were able to confirm our previous statement[18,42,44,45] that the saturating content of Chol keeps the physical properties of the PL bilayer portion of lens lipid membranes constant and independent of changes in the PL composition that occur with age. The lack of protein turnover in the matured fiber cells indicates that integral membrane proteins (mainly aquaporins and connexins), which were synthesized during embryogenesis, should perform the same functions in old lenses that they performed just after synthesis. Thus, the stability and constancy of the physical properties of the PL bilayer portion of lens lipid membranes help to maintain the fiber-cell membrane homeostasis during age-related changes of the PL composition without altering functions of integral proteins.[29,46] Only the properties of pure CBDs changed significantly with the age of the donor. The size of CBDs increased significantly with the age of the donor. Our results also indicate that these changes were determined mainly by the Chol content in the investigated membranes.

Materials and Methods

2.1. Materials

Phospholipid spin labels (*n*-PC, *n* = 5, 7, 10, 12, 14, or 16; T-PC) were obtained from Avanti Polar Lipids, Inc. (Alabaster, AL). Chol-analogue spin labels (CSL and ASL) along with the 9-doxylstearic acid spin labels (9-SASL) were purchased from Molecular Probes (Eugene, OR). See Fig. 1 for spin-label structures.

2.2. Isolation of total lipids from the cortical and nuclear fiber cell membranes of human eye lenses and analysis of lipid composition

Eighteen clear human lenses for each age group 0–20 and 21–40 years were obtained from the Lions Eye Bank of Wisconsin (Madison, WI). Lenses were removed *in situ* from refrigerated bodies within an average time frame of nine hours postmortem. All of the lenses were stored at −80°C until membrane isolations were performed. Lenses were examined using a binocular microscope and were evaluated for color and opacities to determine the presence or absence of cataractous changes. The presence or absence of cataracts was determined by an ophthalmologist using a subjective grading system based on the amount of “yellowness” to the lens (for nuclear cataracts) and opacities (for cortical cataracts). Lenses not demonstrating any of these changes were determine to be free of cataracts. The cortical and nuclear regions of the lenses were separated based on differences in tissue consistency,[13,47] and lipids were extracted separately from each region using the Folch procedure.[48] These procedures were described previously.[49]

Lipids were sent to Avanti Polar Lipids, Inc. (Alabaster, AL), for analysis of the total Chol/PL ratio using high-performance liquid chromatography. Chol/PL ratios for the cortex and nucleus samples of clear lenses of the age group 0–20 years were found to be 0.63 and 0.71, respectively. Similarly, Chol/PL ratios for cortex and nucleus samples of clear lenses of the age group 21–40 years were found to be 1.01 and 1.21, respectively. These values were calculated for the total lipid extracts, thus including lipids from plasma membranes and lipids presented in the cytoplasm. There is evidence that multilamellar bodies presented in the cytoplasm of human aged and cataractous lenses (with a core of crystallin cytoplasm covered by multiple lipid bilayers)[50–53] contain Chol,[54,55] which may affect the Chol/PL molar ratio in plasma membranes calculated based on the total lipid extraction. These effects should be especially pronounced in fiber cells from donors with nuclear cataracts.[52,53,56]

2.3. Preparation of samples for EPR

The membranes were prepared using the rapid solvent exchange method[57–59] with the apparatus that was built in our lab,[60] as described in detail in[57]. The membrane suspensions (containing ~1 mol% spin label) were centrifuged briefly (12000 g, 15 min, 4°C), and the loose pellets were transferred to capillaries and used for electron paramagnetic resonance (EPR) measurements.[61]

2.4. EPR measurements

Conventional EPR spectra were recorded with a Bruker EMX spectrometer. The order parameter was calculated based on spectral parameters measured directly from the spectra

with the precision of ± 0.25 G (see[62 and63] for details). To measure hydrophobicity, the *z*-component of the hyperfine interaction tensor of the *n*-PC, A_Z, was determined from the EPR spectra for samples frozen at −165°C, as described in.[64,65] Values of $2A_Z$ were measured within the precision of ±0.25 G.

Spin-lattice relaxation times, T_1s, of spin labels were obtained from the saturation recovery (SR) signal of the central line measured at X-band.[66] T_1s for membrane fluidity profiles were determined for thoroughly deoxygenated samples.[63] The oxygen transport parameter (OTP) was measured as described previously.[61,67] For measurement of the nickel (II) ethylenediamineN,N′-diacetic acid (NiEDDA) accessibility parameter, a 20 mM NiEDDA was present in the buffer, and SR measurements were performed for deoxygenated samples.[68] SR signals were fitted by single- or double-exponential functions, and T_1s were assigned to a proper membrane environment. The uncertainties in the measurements of decay time from the fits were usually less than 0.05%. For the sample to sample measurements, the single exponential fit was satisfactory within 3% whereas the double exponential fit was satisfactory within 5% for longer and 10% for shorter recovery time constants.

Results and Discussion

The studies discussed here are a continuation of our previously published work on the properties of human lens lipid membranes of donors older than 41 years.[18,42] As such, we will present only the final profiles of membrane properties, with a minimal amount of details as to how certain membrane properties were measured. Detailed methods can be found in the published paper.[42] The work presented here was performed on lens lipid membranes prepared from the total lipids extracted from the clear lens cortices and nuclei of donors from age groups 0–20 and 21–40 years; it is compared with previously obtained data for clear cortical and nuclear membranes of age groups 41–60 and 61–70 years.

3.1. Profiles of membrane properties across PCDs

Similar to our previous work, in this study we used PL- and Chol-analogue spin labels that, when incorporated into membranes, locate the monitoring group, free-radical nitroxide moiety, at a certain depth and in a specific membrane domain (Fig. 1). The EPR signals coming from the monitoring group provide parameters that describe significant membrane properties. These properties include the order[62] and rotational motion[63] of the fragment of acyl chains to which the monitoring group is attached. They also include local membrane properties, around the monitoring group, such as the oxygen diffusion-concentration product[63] and hydrophobicity.[65] The EPR approaches that have been developed allow these parameters to be obtained in homogenous (one phase) lipid bilayers.[69] Some of the data obtained can provide information regarding coexisting domains[70] or phases.[69] The location of the monitoring group at different depths in the lipid bilayer allows these data to be presented as profiles across a membrane. These approaches were successfully used in our studies of lens lipid membranes in which CBDs were induced by high Chol content.[18,42,44,45] We also applied them to intact human[40,71] and porcine[44] membranes with domains induced by integral membrane proteins.

In the studies reported here, we present profiles across human lens lipid membranes from donors of two age groups, namely 0–20 and 21–40 years. In order to demonstrate the meaning and significance of these new data, we have presented the new data along with profiles for age groups 41–60 and 61–70 years, taken from Ref.[42] and Ref.[18], respectively. Profiles describing order and rotational motion of acyl chains are presented in Figs. 2 and 3. Profiles describing oxygen diffusion-concentration products and hydrophobicity are presented in Figs. 4 and 5. Figure 4 contains profiles across coexisting domains, PCD and pure CBD. The PCD is the phospholipid-cholesterol membrane saturated with Chol before formation of the CBD or the PCD coexisting with the CBD. (See[60] for more explanation.)

In human lens lipid membranes, in which CBDs are formed for all age groups, the phospholipid-analogue spin labels should be located only in the bulk PCD, while the Chol analogues should be located in both PCD and CBD.[68] Thus, only Chol-analogue spin labels can discriminate coexisting PCDs and CBDs (Sect. 3.2). However, the location of phospholipid-analogue spin labels in only the PCD ensures that obtained profiles of the order parameter (Sect. 3.1.1), fluidity (Sect. 3.1.2), OTP (Sect. 3.1.3), and hydrophobicity (Sect. 3.1.4) are not “contaminated” by the coexisting CBD.

3.1.1. Acyl chain order—Profiles of the order parameter across the PCD of cortical and nuclear lens lipid membranes obtained from donors of different age groups are presented in Figs. 2A and 2B, respectively. The order parameter should be considered nondynamic because it describes only the amplitude of the wobbling motion of acyl chains.[62] We use the order parameter to describe the depth-dependent acyl chain organization but not fluidity (motion).

As presented in Fig. 2, profiles of the order parameter are all identical. They are identical for all age groups in cortical (Fig. 2A) and nuclear (Fig. 2B) membranes and between cortical and nuclear membranes. As indicated in Sect. 2.2, these membranes differ significantly in Chol content. However, common to all of these membranes is the fact that the Chol content is always high enough to saturate the PL bilayer. This is confirmed by the presence of the CBD in all preparations (Sect 3.2). Profiles of the order parameter for membranes with a saturating amount of Chol, including those presented in Fig. 2, differ from profiles across membranes without Chol.[72] For membranes saturated with Chol, the measured values of the order parameter are always greater than those measured for membranes without Chol. We can conclude that the ordering effect of Chol in lens lipid membranes was observed at all depths from the membrane surface to the membrane center (but see Sect. 3.1.2).

3.1.2. Acyl chain motion—The SR EPR approach makes it possible to measure the spin-lattice relaxation rate (T_1^{-1}) directly from the SR signal. In deoxygenated samples, this spectral parameter depends mainly on the rotational motion of the monitoring group (free-radical nitroxide moiety),[73,74] and, thus, describes motion of the acyl chain fragment to which the nitroxide moiety is attached. We used this conventional way to describe membrane fluidity as the profiles of T_1^{-1} versus depth in the membrane. These fluidity profiles across the PCD of cortical and nuclear lens lipid membranes obtained from clear lenses from donors of different age groups are presented in Fig. 3. As expected, membrane fluidity increases toward the center of all membranes (as indicated by an increase in T_1^{-1}).

Similar to profiles of the order parameter, fluidity profiles in cortical (Fig. 3A) and nuclear (Fig. 3B) lens lipid membranes are practically identical; they also are identical for all age groups. We would like to stress again that all of these similarities are independent of the drastic changes in the human fiber cell membrane PL composition that occur during aging.[5–9,12,13,43]

For simple model membranes, dynamic parameters (T_1^{-1}, rate of rotational motions, OTP) reveal that Chol has a rigidifying effect on acyl chains only to the depth to which the rigid steroid ring is immersed into the lipid bilayer and a fluidizing effect at deeper locations.[30,63,75] As indicated in Sect. 3.1.1, profiles of the order parameter show the ordering effect of Chol at all depths. Similarly, for membranes made from PL mixtures, which resemble the composition of membranes from human lenses, Chol decreases membrane fluidity to the depth of C9 and increases membrane fluidity at deeper locations; these effects cannot be discriminated by profiles of the order parameter.[63] All of these data suggest that, also in human lens lipid membranes, Chol decreases membrane fluidity to the depth at which the Chol rigid ring structure is immersed in the membrane, while the fluidity of acyl chains is increased at deeper locations.

3.1.3. Profiles of the oxygen transport parameter (oxygen diffusion-concentration product)—The OTP[67], which is proportional to the local oxygen diffusion-concentration product, was first used to calculate the oxygen permeability coefficient across model[66] and biological[76] membranes. Soon, we recognized that this parameter describes with great sensitivity (i.e., atomic resolution)[69] the membrane dynamics reported in terms of motion of molecular oxygen. The OTP can be measured simultaneously in coexisting membrane domains and membrane phases. Because of that, it provides a powerful tool for the discrimination of membrane domains[70] and phases.[69] We call these approaches “discrimination by oxygen transport.” We used the OTP as a tool for discrimination of membrane domains (PCD and CBD, see Sect. 3.2) and as a measure of membrane dynamics at different membrane depths (in PCD, this section).

Profiles of the OTP across the bulk PCD of cortical and nuclear lens lipid membranes, obtained with PL spin labels, for all age groups are presented in Fig. 4. Similar to profiles of the order parameter and the T_1^{-1}, profiles of the OTP in cortical and nuclear lens lipid membranes are practically identical; also, they are identical for all age groups. They have a rectangular shape with an abrupt increase in the OTP between the C9 and C10 positions. The abrupt increase that occurs within one carbon-carbon bond (1.3 Å) allows us to state that this method has atomic resolution. Also, the overall change of the OTP across the membrane, which is as large as eight times, confirms the high sensitivity of this approach. In the polar headgroups and in the hydrocarbon region to the depth of C9, the OTP was as low as in gel-phase membranes. At locations deeper than C9, it was as high as in fluid-phase membranes.[66] These profiles are typical for lipid bilayers saturated with Chol and are very different from the bell-shaped profile across membranes without Chol.[69]

3.1.4. Profiles of hydrophobicity—Figure 5 shows rectangular hydrophobicity profiles across the PCD of investigated lens lipid membranes. This rectangular shape is characteristic of lipid bilayer membranes saturated with Chol.[64] The hydrophobicity profiles across lipid

bilayers without Chol have a bell shape with significantly lower hydrophobicity in the membrane center.[64,72] In membranes without Chol, the hydrophobicity of the membrane interior strongly depends on the degree of unsaturation of PL acyl chains.[64,72]

The $2A_Z$ values measured in the center of all membranes (positions from 10-PC to 16-PC in Fig. 5) can be related to the hydrophobicity (or ε) of hexane and dipropylamine (ε = 2.0–2.9), and hydrophobicity near the membrane surface (position of 5-PC in Fig. 5) can be related to that of methanol and ethanol (ε = 24.3–32.6). This is possible by referring to Fig. 2 in the reference[64]. The bulk aqueous phase has a dielectric constant of ε = 80, and, thus, is considerably more polar than all membrane regions. The abrupt increase of hydrophobicity between C9 and C10 also was observed for all lens lipid membranes made from lipids isolated from eye lenses of different species.[42,44,45]

Similar to the profiles of the order parameter (Fig. 2), the T_1^{-1} (Fig. 3), and the profiles of the OTP (Fig. 4), the hydrophobicity profiles were practically identical in all of these membranes, independent of their age group and location within the lens. All of these profiles revealed that mainly the saturating amount of Chol and not the PL composition determines these physical membrane properties.

3.1.5. Measurements in the headgroup region and aqueous phase—Profiles presented in Figs. 3, 4, and 5 contain data obtained for the membrane headgroup region, and profiles in Figs. 4 and 5 contain data from the aqueous phase, outside the membrane. These points gave additional information about measured properties in those regions. Only in the case of the OTP, which describes the collision rate of oxygen with the nitroxide moiety, can the values presented for the hydrocarbon phase be directly compared with those in the headgroup region and in the aqueous phase. It follows from fact that collisions with molecular oxygen are substantially independent of the structure of the nitroxide moiety.[77] In other cases, the chemical structure itself affects the T_1^{-1} of the nitroxide moiety[78,79] as well as the $2A_Z$ value of its EPR spectrum.[80] However, changes in the T_1^{-1} and $2A_Z$ values reflect changes in the fluidity and hydrophobicity, respectively, in the polar headgroup region. When appropriate, measured values in the aqueous phase also were included for comparison with profiles across membranes.

3.2. Discrimination of membrane domains

As we stated in the beginning of Sect. 3.1.1, only Chol analogue spin labels can discriminate the CBD formed within the PCD.[68] The OTP measured with ASL in the center of the CBD was a few times smaller than that measured in the center of the surrounding PL bilayer (Fig. 6). Similarly, the NiEDDA accessibility parameter, measured with CSL located at the membrane-water interface, was a few times greater in the CBD than in the surrounding PL bilayer (Fig. 7). (See Fig. 1 for ASL and CSL chemical structures and approximate locations of their nitroxide moieties in the membrane center and at the membrane surface [at the membrane water interface].) These differences were easily detected using the SR EPR approach, confirming the presence of CBDs in all investigated cortical and nuclear membranes.

3.2.1. Age-related changes—Obtained with ASL and CSL, values of the OTP are included in the profiles presented in Fig. 4. A correct assignment of the SR data for ASL is confirmed by the fact that one of the two OTP values fits into the profile across the PCD, thus coming from ASL molecules located in this domain. The other value was assigned to the CBD. As indicated below (measurements with NiEDDA), CSL is also located in these two environments. However, the OTP cannot discriminate these locations, giving the same values in the PCD and the CBD (see Ref.[81] for more details). Values obtained with ASL and CSL in the CBD allowed us to draw approximate profiles (straight lines connecting experimental points) of the OTP across this domain (Fig. 4). Data presented in Fig. 4 indicate that the OTP (measured with ASL) in the CBD differs significantly between membranes from different age groups and between cortical and nuclear membranes from the same age groups. To better describe these age and spatial dependences, we constructed Fig. 6A; in this figure, the OTP values obtained with ASL in PCD and CBD for cortical and nuclear lens lipid membranes are plotted as a function of the ages of the donors. Results are presented for cortical and nuclear lens lipid membranes isolated from a pool of 18 clear human lenses in each of two different age groups (0–20 and 21–40 years) investigated in the presented work and recently published results for donors from the age groups 41–60 and 61–70 years.

Fig. 6A demonstrates that, as expected and as described in Sect. 3.1.3, values of the OTP measured in the PCD are independent of the age of the donor and are the same in cortical and nuclear membranes. However, values measured in the CBD decrease with the age of the donor, and values at all ages are smaller in nuclear membranes as compared to those measured in cortical membranes. OTPs measured in the CBD for donors from the age group 0–20 years were about 33% smaller than that those measured in the PCD. For donors from the age group 61–70 years, the values in the CBD were ~5.5 times smaller than those measured in the PCD. The difference between both domains increases with the age of the donor but somewhat levels out for the last two age groups.

In Fig. 7A, the NiEDDA accessibility parameter values obtained with CSL in the CBD and PCD for cortical and nuclear lens lipid membranes were plotted as a function of the age of the donor. Results obtained in this investigation, together with those recently published, are presented. Similar to the OTP, the values of the NiEDDA accessibility parameter measured in the PCD were substantially independent of the age of the donor and were very close in cortical and nuclear membranes. Again, the difference between values measured in the CBD and the PCD increases with the age of the donor and levels out for donors older than 40 years. Also, values measured in the CBD of cortical membranes were closer to those measured in the PCD than to those measured in the CBD and PCD of nuclear membranes.

3.2.2. Changes as a function of cholesterol content—The OTP and NiEDDA accessibility parameter sensed by ASL and CSL, respectively, in the CBD are the only properties that can be assigned to the CBD. We showed that, in model membranes, these properties change significantly with Chol content. They were close to the properties in the surrounding PCD at low Chol content when CBDs start to form, and the difference increases with Chol content[60]. This suggests that the increased Chol content reduced the effect of the surrounding PCD on the properties of the CBD. Most likely, this is the result of the increase

in the size of the individual CBD. To better describe these Chol dependencies, we constructed Figs. 6B and 7B, where the OTP values obtained with ASL in PCD and CBD (Fig. 6B) and the NiEDDA accessibility parameter values obtained with CSL in PCD and CBD (Fig. 7B) are presented as a function Chol content in investigated membranes. Chol contents in the investigated lens lipid membranes are listed in Sect. 2.2 for donors from the age groups 0–20 and 21–40 years, in Sect. 2.2 of the reference[42] for donors from the age group 41–60 years, and in the section titled *Isolation of total lipids from the cortical and nuclear fiber cell membranes of human eye lenses and analysis of lipid composition* of the reference[18] for donors from the age group 61–70 years.

Both figures (Fig. 6B and Fig. 7B) reveal that all observed age and spatial differences, described in Sect. 3.2.1, were due to changes in Chol content in the investigated membranes. Membrane Chol content changes with age and was different in cortical and nuclear membranes. After that "correction," all observed abrupt differences collapsed to a smooth function of Chol content. Based on these data, we can conclude that properties of pure CBDs changed significantly with the age of the donor and were related to the size of the CBD, which increased with the age of the donor and was always greater in the nuclear than in the cortical membranes. Also, the above analysis revealed that the size of the CBD was determined mainly by the Chol content in the investigated membranes.

Conclusions

In summary, our conclusions are as follows: (1) CBDs are present in both cortical and nuclear lens lipid membranes, independent of the age of donor. (2) Because of the presence of CBDs, the PL-Chol bilayer (we call it PCD) is always saturated with Chol. (3) The physical properties of the PCD are practically identical for cortical and nuclear membranes and are the same for all age groups. (4) Properties of pure CBDs change significantly with the age of the donor and are related to the size of the CBD, which increases with the age of the donor and is always greater in nuclear than in cortical membranes. (5) The size of the CBD is determined mainly by the Chol content in the investigated membranes. (6) The Chol content at which CBDs start to form depends on the PL composition of the investigated membranes (see reference[30] for a more-detailed explanation of this dependence). (7) The Chol content (expressed as Chol/PL molar ratio) in cortical and nuclear lens lipid membranes increases almost linearly with the age of the donor, up to the Chol solubility threshold (i.e., the Chol content at which Chol crystals start to form, at a Chol/PL molar ratio of ~2 in the investigated membranes). (8) The difference between Chol content in cortical and nuclear membranes is negligible in lenses from young donors. This difference increases significantly with the age. (9) Excess Chol above the Chol solubility threshold results in the formation of Chol crystals that do not affect the properties of lens lipid membranes.

Our conclusions are depicted in Figure 8, which presents changes in the organization of cortical and nuclear lens lipid membranes as a function of age and Chol content. Figure 8 does not include age-related changes in PL composition,[5–9,12,13,43] which also affect the organization and properties of lens lipid membranes and should alter the functions of integral membrane proteins.[82–85] Independent of age, the amount of Chol in fiber cell

membranes is always high enough to saturate the PL bilayer, or even oversaturate it, allowing the formation of the CBD or even Chol crystals. This saturating Chol content and the presence of CBDs ensures that the physical properties of the PCD do not change significantly during the aging process[18,42] and that membrane integral proteins are always surrounded by the lipid bilayer with the same physical properties. Thus, lipid composition and lipid organization appear to help to maintain fiber cell membrane homeostasis. It needs to be pointed out that the PL composition determines the Chol concentration at which CBDs are formed.[30] Interestingly, in that delicate balance, the age-related changes in the PL composition delay the age (increase the Chol content) at which CBDs are formed. (See Refs.[4,30] for further discussions.) This is also expressed in Fig. 8, where the CBD is shown at Chol/PL molar ratios of ~0.6 and ~2.0 in the lens lipid membranes of young and aged donors, respectively. Such an observation is in agreement with the preferential depletion of glycerolphospholipids in older fiber cells and the subsequent enrichment of sphingolipids, mainly in dihydrosphingolipids.[7,10] It seems that this balance plays an integral role in maintaining the homeostasis of the fiber-cell plasma membrane, the fiber cell itself, the whole lens, and, thus, lens transparency.[5]

Acknowledgments

This work was supported by grants EY001931 and EY015526 from the National Institutes of Health. We acknowledge the help of Bhavna P. Sheth, MD, MBA. Thanks to the Lions Eye Bank of Wisconsin for obtaining the human lenses used in this study.

References

1. Bassnett S, Shi Y, Vrensen GF. Biological glass: structural determinants of eye lens transparency. Philos Trans Royal Soc Lond Ser B Biol Sci. 2011; 366:1250–1264.
2. Rafferty, NS. Lens morphology. In: Maisel, H., editor. The ocular lens:structure, function and pathology. New York: Marcel Dekker; 1985. p. 1-60.
3. Wride MA. Lens fibre cell differentiation and organelle loss: many paths lead to clarity. Philos Trans Royal Soc Lond Ser B Biol Sci. 2011; 366:1219–1233.
4. Deeley JM, Mitchell TW, Wei X, Korth J, Nealon JR, Blanksby SJ, et al. Human lens lipids differ markedly from those of commonly used experimental animals. Biochim Biophys Acta. 2008; 1781:288–298. [PubMed: 18474264]
5. Huang L, Grami V, Marrero Y, Tang D, Yappert MC, Rasi V, et al. Human lens phospholipid changes with age and cataract. Invest Ophthalmol Vis Sci. 2005; 46:1682–1689. [PubMed: 15851569]
6. Paterson CA, Zeng J, Husseini Z, Borchman D, Delamere NA, Garland D, et al. Calcium ATPase activity and membrane structure in clear and cataractous human lenses. Curr Eye Res. 1997; 16:333–338. [PubMed: 9134322]
7. Yappert MC, Rujoi M, Borchman D, Vorobyov I, Estrada R. Glycero- versus sphingo-phospholipids: correlations with human and non-human mammalian lens growth. Exp Eye Res. 2003; 76:725–734. [PubMed: 12742355]
8. Truscott RJ. Age-related nuclear cataract: a lens transport problem. Ophthalmic Res. 2000; 32:185–194. [PubMed: 10971179]
9. Borchman D, Byrdwell WC, Yappert MC. Regional and age-dependent differences in the phospholipid composition of human lens membranes. Invest Ophthalmol Vis Sci. 1994; 35:3938–3942. [PubMed: 7928192]
10. Yappert MC, Borchman D. Sphingolipids in human lens membranes: an update on their composition and possible biological implications. Chem Phys Lipids. 2004; 129:1–20. [PubMed: 14998723]

11. Li LK, So L, Spector A. Membrane cholesterol and phospholipid in consecutive concentric sections of human lenses. J Lipid Res. 1985; 26:600–609. [PubMed: 4020298]
12. Li LK, So L, Spector A. Age-dependent changes in the distribution and concentration of human lens cholesterol and phospholipids. Biochim Biophys Acta. 1987; 917:112–120. [PubMed: 3790601]
13. Rujoi M, Jin J, Borchman D, Tang D, Yappert MC. Isolation and lipid characterization of cholesterol-enriched fractions in cortical and nuclear human lens fibers. Invest Ophthalmol Vis Sci. 2003; 44:1634–1642. [PubMed: 12657603]
14. Zelenka PS. Lens lipids. Curr Eye Res. 1984; 3:1337–1359. [PubMed: 6391828]
15. Jacob RF, Cenedella RJ, Mason RP. Direct evidence for immiscible cholesterol domains in human ocular lens fiber cell plasma membranes. J Biol Chem. 1999; 274:31613–31618. [PubMed: 10531368]
16. Jacob RF, Cenedella RJ, Mason RP. Evidence for distinct cholesterol domains in fiber cell membranes from cataractous human lenses. J Biol Chem. 2001; 276:13573–13578. [PubMed: 11278611]
17. Mason R, Tulenko TN, Jacob RF. Direct evidence for cholesterol crystalline domains in biological membranes: role in human pathobiology. Biochim Biophys Acta. 2003; 1610:198–207. [PubMed: 12648774]
18. Mainali L, Raguz M, O'Brien WJ, Subczynski WK. Properties of membranes derived from the total lipids extracted from clear and cataractous lenses of 61–70-year-old human donors. Eur Biophys J. 2015; 44:91–102. [PubMed: 25502634]
19. Tulenko TN, Chen M, Mason PE, Mason RP. Physical effects of cholesterol on arterial smooth muscle membranes: evidence of immiscible cholesterol domains and alterations in bilayer width during atherogenesis. J Lipid Res. 1998; 39:947–956. [PubMed: 9610760]
20. Leuschen J, Mortensen EM, Frei CR, Mansi EA, Panday V, Mansi I. Association of statin use with cataracts: a propensity score-matched analysis. JAMA ophthalmology. 2013; 131:1427–1434. [PubMed: 24052188]
21. Lai CL, Shau WY, Chang CH, Chen MF, Lai MS. Statin use and cataract surgery: a nationwide retrospective cohort study in elderly ethnic Chinese patients. Drug Saf. 2013; 36:1017–1024. [PubMed: 23771795]
22. Machan CM, Hrynchak PK, Irving EL. Age-related cataract is associated with type 2 diabetes and statin use. Optom Vis Sci. 2012; 89:1165–1171. [PubMed: 22797512]
23. Hippisley-Cox J, Coupland C, Brindle P. The performance of seven QPrediction risk scores in an independent external sample of patients from general practice: a validation study. BMJ open. 2014; 4:e005809.
24. Duewell P, Kono H, Rayner KJ, Sirois CM, Vladimer G, Bauernfeind FG, et al. NLRP3 inflammasomes are required for atherogenesis and activated by cholesterol crystals. Nature. 2010; 464:1357–1361. [PubMed: 20428172]
25. Tang D, Borchman D, Yappert MC, Cenedella RJ. Influence of cholesterol on the interaction of alpha-crystallin with phospholipids. Exp Eye Res. 1998; 66:559–567. [PubMed: 9628803]
26. Tang D, Borchman D, Yappert MC. Alpha-crystallin/lens lipid interactions using resonance energy transfer. Ophthalmic Res. 1999; 31:452–462. [PubMed: 10474075]
27. Boyle DL, Takemoto L. EM immunolocalization of alpha-crystallins: association with the plasma membrane from normal and cataractous human lenses. Curr Eye Res. 1996; 15:577–582. [PubMed: 8670759]
28. Cenedella RJ, Fleschner CR. Selective association of crystallins with lens 'native' membrane during dynamic cataractogenesis. Curr Eye Res. 1992; 11:801–815. [PubMed: 1424724]
29. Subczynski WK, Mainali L, Raguz M, O'Brien WJ. Organization of Lipids in Fiber-Cell Plasma Membranes of the Eye Lens. Exp Eye Res. 2016; doi: 10.1016/j.exer.2016.03.004
30. Subczynski WK, Raguz M, Widomska J, Mainali L, Konovalov A. Functions of cholesterol and the cholesterol bilayer domain specific to the fiber-cell plasma membrane of the eye lens. J Membr Biol. 2012; 245:51–68. [PubMed: 22207480]
31. Gonen T, Cheng Y, Kistler J, Walz T. Aquaporin-0 membrane junctions form upon proteolytic cleavage. J Mol Biol. 2004; 342:1337–1345. [PubMed: 15351655]

32. Kistler J, Bullivant S. Lens gap junctions and orthogonal arrays are unrelated. FEBS Lett. 1980; 111:73–78. [PubMed: 7358167]
33. Buzhynskyy N, Hite RK, Walz T, Scheuring S. The supramolecular architecture of junctional microdomains in native lens membranes. EMBO Rep. 2007; 8:51–55. [PubMed: 17124511]
34. Costello MJ, McIntosh TJ, Robertson JD. Distribution of gap junctions and square array junctions in the mammalian lens. Invest Ophthalmol Vis Sci. 1989; 30:975–989. [PubMed: 2722452]
35. Dunia I, Cibert C, Gong X, Xia CH, Recouvreur M, Levy E, et al. Structural and immunocytochemical alterations in eye lens fiber cells from Cx46 and Cx50 knockout mice. Eur J Cell Biol. 2006; 85:729–752. [PubMed: 16740340]
36. Zampighi GA, Eskandari S, Hall JE, Zampighi L, Kreman M. Micro-domains of AQP0 in lens equatorial fibers. Exp Eye Res. 2002; 75:505–519. [PubMed: 12457863]
37. Biswas SK, Lee JE, Brako L, Jiang JX, Lo WK. Gap junctions are selectively associated with interlocking ball-and-sockets but not protrusions in the lens. Mol Vis. 2010; 16:2328–2341. [PubMed: 21139982]
38. Biswas SK, Lo WK. Gap junctions contain different amounts of cholesterol which undergo unique sequestering processes during fiber cell differentiation in the embryonic chicken lens. Mol Vis. 2007; 13:345–359. [PubMed: 17392685]
39. Biswas SK, Jiang JX, Lo WK. Gap junction remodeling associated with cholesterol redistribution during fiber cell maturation in the adult chicken lens. Mol Vis. 2009; 15:1492–1508. [PubMed: 19657477]
40. Raguz M, Mainali L, O'Brien WJ, Subczynski WK. Lipid domains in intact fiber-cell plasma membranes isolated from cortical and nuclear regions of human eye lenses of donors from different age groups. Exp Eye Res. 2015; 132:78–90. [PubMed: 25617680]
41. Kuszak, JR., Costello, MJ. The Structure of the Vertebrate Lens. In: Lovicu, FJ., Robinson, ML., editors. Development of the Ocular Lens. Cambridge: Cambridge University Press; 2004. p. 71-118.
42. Mainali L, Raguz M, O'Brien WJ, Subczynski WK. Properties of membranes derived from the total lipids extracted from the human lens cortex and nucleus. Biochim Biophys Acta. 2013; 1828:1432–1440. [PubMed: 23438364]
43. Roy D, Rosenfeld L, Spector A. Lens plasma membrane: isolation and biochemical characterization. Exp Eye Res. 1982; 35:113–129. [PubMed: 7151881]
44. Mainali L, Raguz M, O'Brien WJ, Subczynski WK. Properties of fiber cell plasma membranes isolated from the cortex and nucleus of the porcine eye lens. Exp Eye Res. 2012; 97:117–129. [PubMed: 22326289]
45. Raguz M, Widomska J, Dillon J, Gaillard ER, Subczynski WK. Physical properties of the lipid bilayer membrane made of cortical and nuclear bovine lens lipids: EPR spin-labeling studies. Biochim Biophys Acta. 2009; 1788:2380–2388. [PubMed: 19761756]
46. Subczynski WK, Raguz M, Widomska J, Mainali L, Konovalov A. Functions of cholesterol and the cholesterol bilayer domain specific to the fiber-cell plasma membrane of the eye lens. The Journal of membrane biology. 2012; 245:51–68. [PubMed: 22207480]
47. Estrada R, Yappert MC. Regional phospholipid analysis of porcine lens membranes by matrix-assisted laser desorption/ionization time-of-flight mass spectrometry. J Mass Spectrom. 2004; 39:1531–1540. [PubMed: 15578747]
48. Folch J, Lees M, Sloane Stanley GH. A simple method for the isolation and purification of total lipids from animal tissues. J Biol Chem. 1957; 226:497–509. [PubMed: 13428781]
49. Raguz M, Widomska J, Dillon J, Gaillard ER, Subczynski WK. Characterization of lipid domains in reconstituted porcine lens membranes using EPR spin-labeling approaches. Biochim Biophys Acta. 2008; 1778:1079–1090. [PubMed: 18298944]
50. Costello MJ, Johnsen S, Gilliland KO, Freel CD, Fowler WC. Predicted light scattering from particles observed in human age-related nuclear cataracts using mie scattering theory. Invest Ophthalmol Vis Sci. 2007; 48:303–312. [PubMed: 17197547]
51. Gilliland KO, Freel CD, Lane CW, Fowler WC, Costello MJ. Multilamellar bodies as potential scattering particles in human age-related nuclear cataracts. Mol Vis. 2001; 7:120–130. [PubMed: 11435998]

52. Gilliland KO, Freel CD, Johnsen S, Craig Fowler W, Costello MJ. Distribution, spherical structure and predicted Mie scattering of multilamellar bodies in human age-related nuclear cataracts. Exp Eye Res. 2004; 79:563–576. [PubMed: 15381040]
53. Gilliland KO, Johnsen S, Metlapally S, Costello MJ, Ramamurthy B, Krishna PV, et al. Mie light scattering calculations for an Indian age-related nuclear cataract with a high density of multilamellar bodies. Mol Vis. 2008; 14:572–582. [PubMed: 18385793]
54. VanMarle J, Vrensen GFJM. Cholesterol Content of Focal Opacities and Multilamellar Bodies in the Human Lens: Filipin Cytochemistry and Freeze Fracture. Ophthalmic Res. 2000; 32:285–291. [PubMed: 11015040]
55. Duindam JJ, Vrensen GF, Otto C, Greve J. Cholesterol, phospholipid, and protein changes in focal opacities in the human eye lens. Invest Ophthalmol Vis Sci. 1998; 39:94–103. [PubMed: 9430550]
56. Costello MJ, Burette A, Weber M, Metlapally S, Gilliland KO, Fowler WC, et al. Electron tomography of fiber cell cytoplasm and dense cores of multilamellar bodies from human age-related nuclear cataracts. Exp Eye Res. 2012; 101:72–81. [PubMed: 22728317]
57. Buboltz JT. A more efficient device for preparing model-membrane liposomes by the rapid solvent exchange method. Rev Sci Instrum. 2009; 80:124301. [PubMed: 20059155]
58. Huang J, Buboltz JT, Feigenson GW. Maximum solubility of cholesterol in phosphatidylcholine and phosphatidylethanolamine bilayers. Biochim Biophys Acta. 1999; 1417:89–100. [PubMed: 10076038]
59. Buboltz JT, Feigenson GW. A novel strategy for the preparation of liposomes: rapid solvent exchange. Biochim Biophys Acta. 1999; 1417:232–245. [PubMed: 10082799]
60. Mainali L, Raguz M, Subczynski WK. Formation of Cholesterol Bilayer Domains Precedes Formation of Cholesterol Crystals in Cholesterol/Dimyristoylphosphatidylcholine Membranes: EPR and DSC Studies. J Phys Chem B. 2013; 117:8994–9003. [PubMed: 23834375]
61. Subczynski WK, Felix CC, Klug CS, Hyde JS. Concentration by centrifugation for gas exchange EPR oximetry measurements with loop-gap resonators. J Magn Reson. 2005; 176:244–248. [PubMed: 16040261]
62. Marsh, D. Electron spin resonance: spin labels. In: Grell, E., editor. Membrane Spectroscopy. Berlin: Springer-Verlag; 1981. p. 51-142.
63. Mainali L, Feix JB, Hyde JS, Subczynski WK. Membrane fluidity profiles as deduced by saturation-recovery EPR measurements of spin-lattice relaxation times of spin labels. J Magn Reson. 2011; 212:418–425. [PubMed: 21868272]
64. Subczynski WK, Wisniewska A, Yin J-J, Hyde JS, Kusumi A. Hydrophobic barriers of lipid bilayer membranes formed by reduction of water penetration by alkyl chain unsaturation and cholesterol. Biochemistry. 1994; 33:7670–7681. [PubMed: 8011634]
65. Griffith OH, Dehlinger PJ, Van SP. Shape of the hydrophobic barrier of phospholipid bilayers (evidence for water penetration in biological membranes). J Membr Biol. 1974; 15:159–192. [PubMed: 4366085]
66. Subczynski WK, Hyde JS, Kusumi A. Oxygen permeability of phosphatidylcholine-cholesterol membranes. Proc Natl Acad Sci USA. 1989; 86:4474–4478. [PubMed: 2543978]
67. Kusumi A, Subczynski WK, Hyde JS. Oxygen transport parameter in membranes as deduced by saturation recovery measurements of spin-lattice relaxation times of spin labels. Proc Natl Acad Sci USA. 1982; 79:1854–1858. [PubMed: 6952236]
68. Raguz M, Mainali L, Widomska J, Subczynski WK. Using spin-label electron paramagnetic resonance (EPR) to discriminate and characterize the cholesterol bilayer domain. Chem Phys Lipids. 2011; 164:819–829. [PubMed: 21855534]
69. Subczynski WK, Wisniewska A, Hyde JS, Kusumi A. Three-dimensional dynamic structure of the liquid-ordered domain as examined by a pulse-EPR oxygen probing. Biophys J. 2007; 92:1573–1584. [PubMed: 17142270]
70. Ashikawa I, Yin J-J, Subczynski WK, Kouyama T, Hyde JS, Kusumi A. Molecular organization and dynamics in bacteriorhodopsin-rich reconstituted membranes: discrimination of lipid environments by the oxygen transport parameter using a pulse ESR spin-labeling technique. Biochemistry. 1994; 33:4947–4952. [PubMed: 8161556]

71. Raguz M, Mainali L, O'Brien WJ, Subczynski WK. Lipid-protein interactions in plasma membranes of fiber cells isolated from the human eye lens. Exp Eye Res. 2014; 120:138–151. [PubMed: 24486794]

72. Mainali L, Raguz M, Subczynski WK. Phases and domains in sphingomyelin-cholesterol membranes: structure and properties using EPR spin-labeling methods. Eur Biophys J. 2012; 41:147–159. [PubMed: 22033879]

73. Robinson BH, Haas DA, Mailer C. Molecular dynamics in liquids: spin-lattice relaxation of nitroxide spin labels. Science. 1994; 263:490–493. [PubMed: 8290958]

74. Mailer C, Nielsen RD, Robinson BH. Explanation of spin-lattice relaxation rates of spin labels obtained with multifrequency saturation recovery EPR. J Phys Chem A. 2005; 109:4049–4061. [PubMed: 16833727]

75. Smith AK, Freed JH. Dynamics and ordering of lipid spin-labels along the coexistence curve of two membrane phases: an ESR study. Chem Phys Lipids. 2012; 165:348–361. [PubMed: 22586732]

76. Subczynski WK, Hopwood LE, Hyde JS. Is the mammalian cell plasma membrane a barrier to oxygen transport? J Gen Physiol. 1992; 100:69–87. [PubMed: 1324973]

77. Hyde, JS., Subczynski, WK. Spin-label oximetry. In: Berliner, LJ., Reuben, J., editors. Biological Magnetic Resonance. New York: Plenum Press; 1989. p. 399-425.

78. Hyde JS, Yin J-J, Subczynski WK, Camenisch TG, Ratke JJ, Froncisz W. Spin-Label EPR T1 Values Using Saturation Recovery from 2 to 35 GHz†. J Phys Chem B. 2004; 108:9524–9529.

79. Froncisz W, Camenisch TG, Ratke JJ, Anderson JR, Subczynski WK, Strangeway RA, et al. Saturation recovery EPR and ELDOR at W-band for spin labels. J Magn Reson. 2008; 193:297–304. [PubMed: 18547848]

80. Berliner, LJ. Appendix II: Principal Values of the g and Hyperfine Tensors of Several Nitroxides Reported to Date. In: Berliner, LJ., editor. Spin Labeling Theory and Applications. New York: Academic Press; 1976. p. 564-565.

81. Raguz M, Mainali L, Widomska J, Subczynski WK. Using spin-label electron paramagnetic resonance (EPR) to discriminate and characterize the cholesterol bilayer domain. Chem Phys Lipids. 2011; 164:819–829. [PubMed: 21855534]

82. Epand, RM. Role of membrane lipids in modulating the activity of membrane-bound enzymes. In: Yeagle, PL., editor. The Structure of Biological Membrane. Boca Raton: CRC Press; 2005. p. 499-509.

83. Reichow SL, Gonen T. Lipid-protein interactions probed by electron crystallography. Curr Opin Struct Biol. 2009; 19:560–565. [PubMed: 19679462]

84. Tong J, Briggs Margaret M, McIntosh Thomas J. Water Permeability of Aquaporin-4 Channel Depends on Bilayer Composition, Thickness, and Elasticity. Biophys J. 2012; 103:1899–1908. [PubMed: 23199918]

85. Tong J, Canty JT, Briggs MM, McIntosh TJ. The water permeability of lens aquaporin-0 depends on its lipid bilayer environment. Exp Eye Res. 2013; 113:32–40. [PubMed: 23680159]

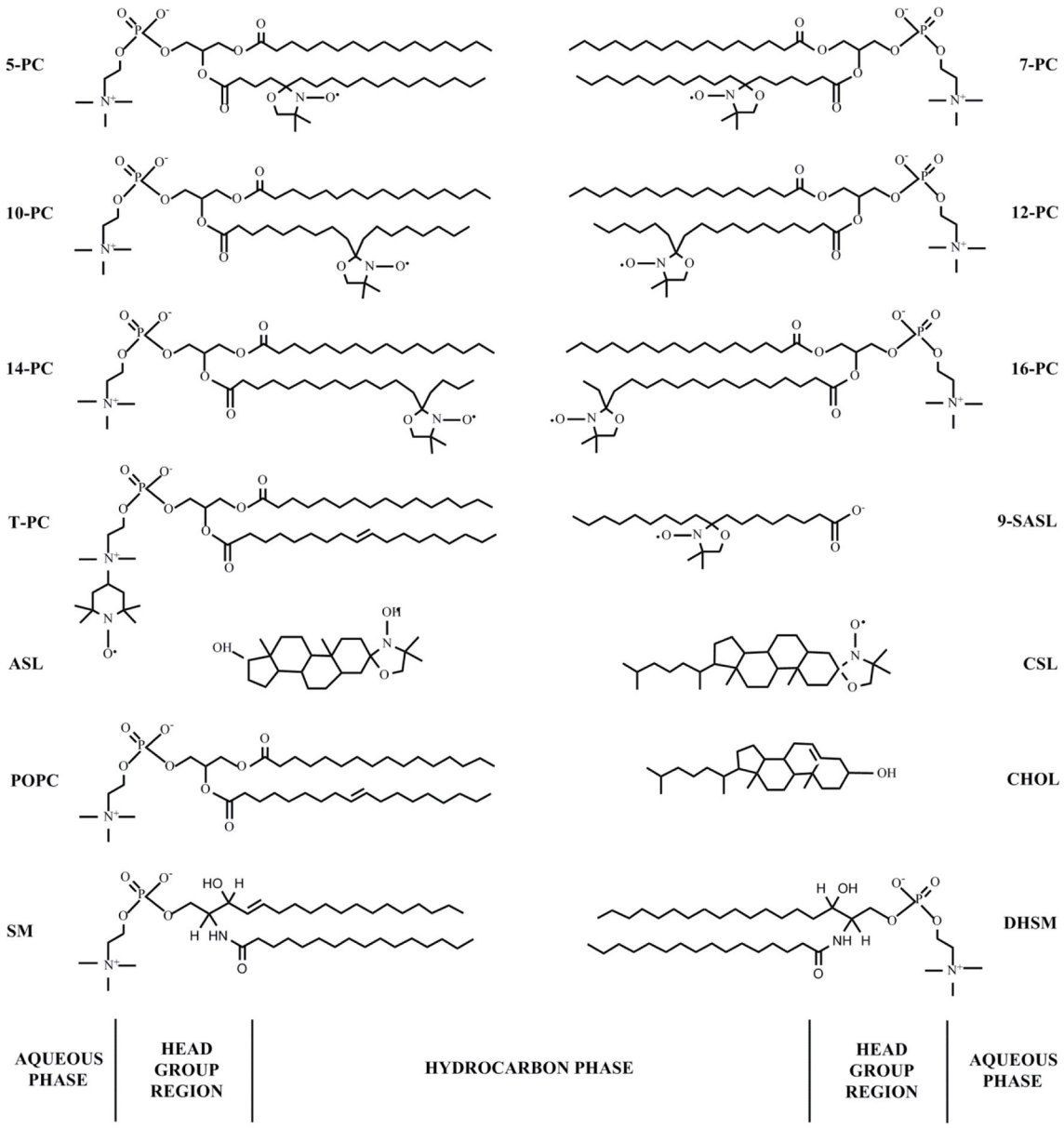

Figure 1.

Chemical structures of phospholipid- (*n*-PCs, T-PC, 9-SASL) and Chol-analogue spin labels (CSL, ASL), together with the structure of phosphatidylcholine (POPC), palmitoyl sphingomyelin (SM) and palmitoyl dihydrosphingomyelin (DHSM) (SM and DHSM are the most abundant phospholipids in human lens membranes), and cholesterol (CHOL). The approximate locations of these molecules across the lipid bilayer membrane are illustrated.

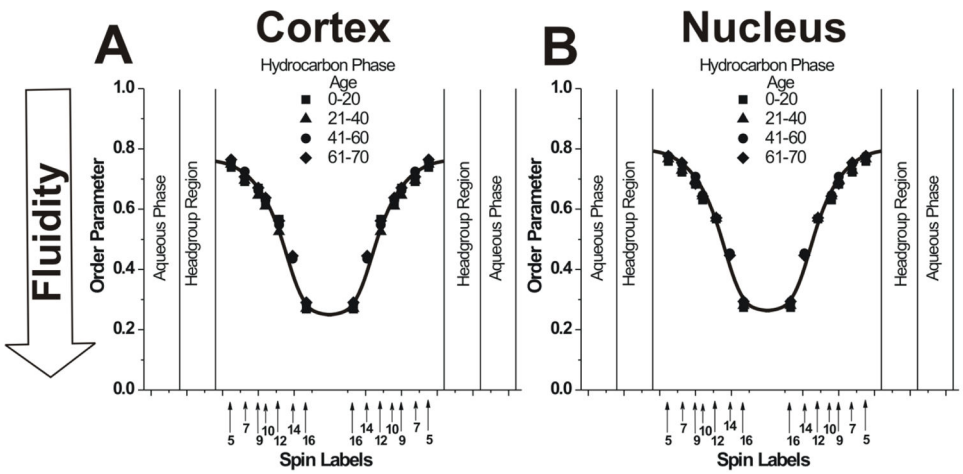

Figure 2.

Profiles of the order parameter obtained at 37°C with phospholipid-analogue spin labels across PCD for cortical (A) and nuclear (B) lens lipid membranes of eye lenses from human donors of different age groups. Data for age groups 41–60 and 61–70 years are reproduced, respectively, from Reference 42, Copyright 2013, with permission from Elsevier, and from Reference 18, Copyright 2014, with permission from Springer Publishing. The approximate localizations of the nitroxide moieties of spin labels are indicated by arrows.

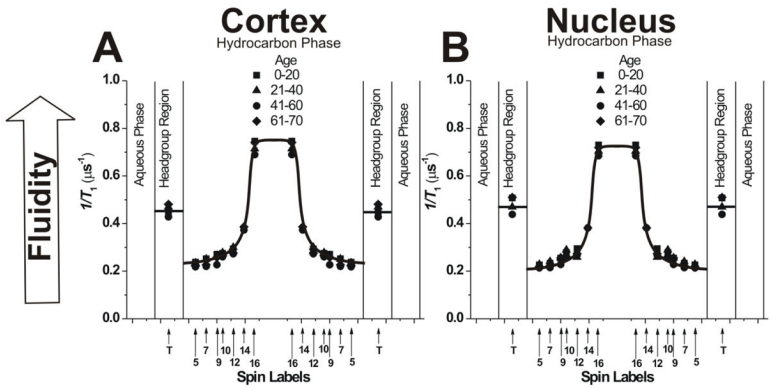

Figure 3.

Fluidity profiles (T_1^{-1} versus depth in the membrane) obtained at 37°C with phospholipid-analogue spin labels across PCD for cortical (A) and nuclear (B) lens lipid membranes of eye lenses from human donors of different age groups. Data for age groups 41–60 and 61–70 years are reproduced, respectively, from Reference 42, Copyright 2013, with permission from Elsevier, and from Reference 18, Copyright 2014, with permission from Springer Publishing. Values in the headgroup region were obtained with the T-PC (T), the nitroxide moiety of which possesses a different chemical structure than nitroxide moieties of other phospholipid-analogue spin labels (Fig. 1). Because of that, values obtained with T-PC cannot be straightforward compared with those obtained in the membrane hydrocarbon phase (see Sect. 3.1.5). The approximate localizations of the nitroxide moieties of spin labels are indicated by arrows.

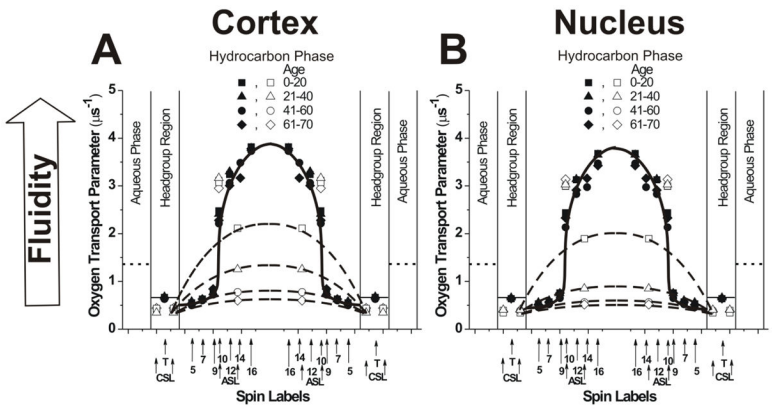

Figure 4.

Profiles of the OTP (the local oxygen diffusion-concentration product) obtained at 37°C with phospholipid- (solid symbols) and Chol-analogue spin labels (open symbols) across PCD (solid lines) and CBD (broken lines) for cortical (A) and nuclear (B) lens lipid membranes of eye lenses from human donors of different age groups. Data for age groups 41–60 and 61–70 years are reproduced, respectively, from Reference 42, Copyright 2013, with permission from Elsevier, and from Reference 18, Copyright 2014, with permission from Springer Publishing. The approximate localizations of the nitroxide moieties of spin labels are indicated by arrows. Localizations of the nitroxide moieties of Chol analogue spin labels of ASL and CSL in the PCD and the CBD are explained in Sect. 3.5 of the reference.[49] The value of the OTP in the aqueous phase also is shown (dotted lines).

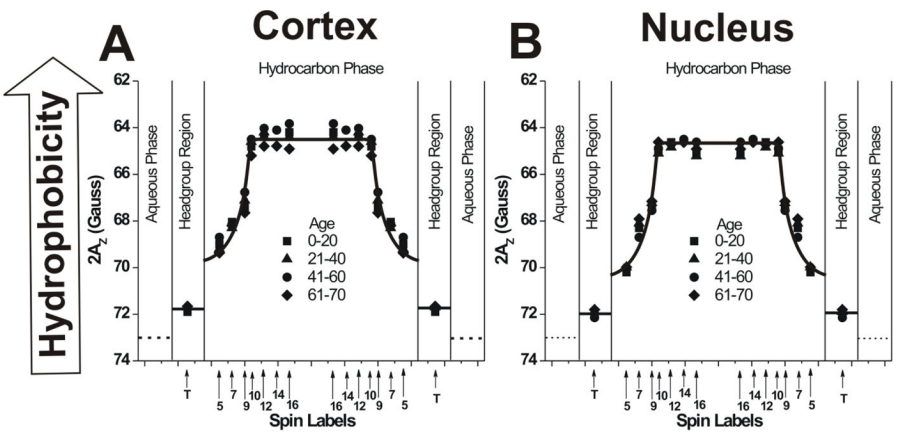

Figure 5.

Hydrophobicity profiles ($2A_Z$ versus depth in the membrane) obtained with phospholipid-analogue spin labels across PCD for cortical (A) and nuclear (B) lens lipid membranes of eye lenses from human donors of different age groups. Data for age groups 41–60 and 61–70 years are reproduced, respectively, from Reference 42, Copyright 2013, with permission from Elsevier, and from Reference 18, Copyright 2014, with permission from Springer Publishing. Values in the headgroup region were obtained with the T-PC (T), the nitroxide moiety of which possesses a different chemical structure than the nitroxide moieties of other phospholipid-analogue spin labels (Fig. 1). Because of that, values obtained with T-PC cannot be straightforward compared with those obtained in the membrane hydrocarbon phase. The $2A_Z$ value in the aqueous phase (a dotted line) was obtained with 16-SASL; thus, it can be straightforward compared with those in the hydrocarbon phase. (See Sect. 3.1.5 for more explanation.) Approximate localizations of the nitroxide moieties of spin labels are indicated by arrows. Smaller $2A_Z$ values indicate higher hydrophobicity (upward changes in the profiles).

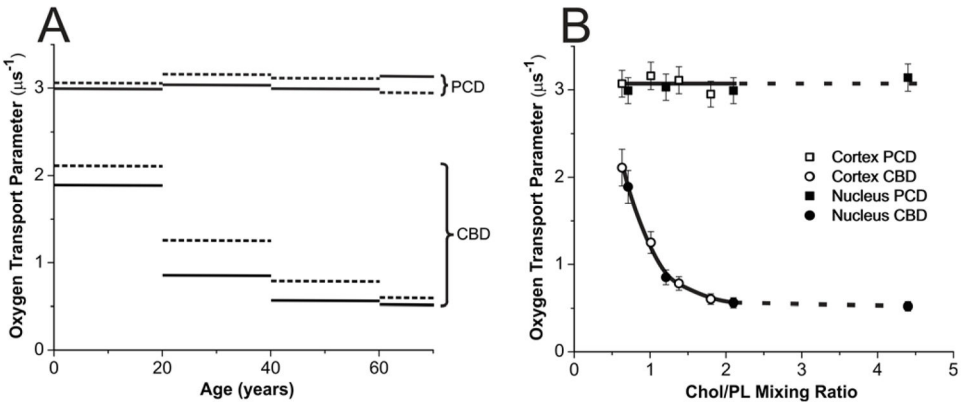

Figure 6.

(A) The OTP obtained with ASL in cortical (dotted lines) and nuclear (solid lines) lens lipid membranes of eye lenses from human donors of different age groups. Data for age groups 41–60 and 61–70 years are reproduced, respectively, from Reference 42, Copyright 2013, with permission from Elsevier, and from Reference 18, Copyright 2014, with permission from Springer Publishing. (B) The same data as in (A) but plotted as a function of the Chol/PL mixing ratio in the suspension of lens lipid membranes. Notice that above the Chol/PL mixing ratio of ~2, the Chol crystals are formed in liposome suspensions. Thus, the Chol/PL molar ratio in PCDs and the amount of Chol forming CBDs should not increase further. Chol crystals form presumably outside the membrane and can be detected by the DSC only after a significant amount of Chol is accumulated in these Chol structures. In our investigations, Chol crystals were detected only for nuclear membranes from the age group 61–70 years with the Chol/PL molar ratio of 4.4. For nuclear membranes from the age group 41–60 years with the Chol/PL molar ratio of 2.1 we were unable to detect Chol crystals.

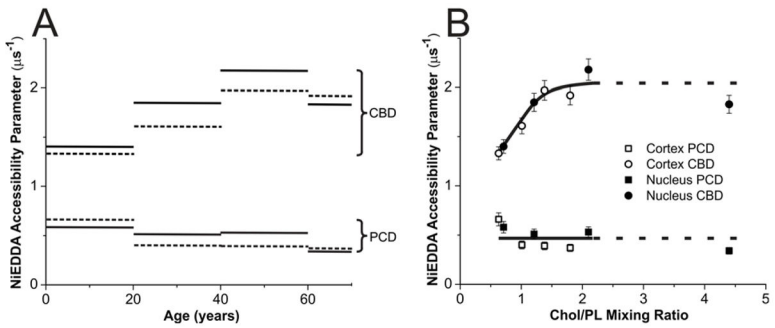

Figure 7.

(A) The NiEDDA accessibility parameter obtained with CSL in cortical (dotted lines) and nuclear (solid lines) lens lipid membranes of eye lenses from human donors of different age groups. Data for age groups 41–60 and 61–70 years are reproduced, respectively, from Reference 42, Copyright 2013, with permission from Elsevier, and from Reference 18, Copyright 2014, with permission from Springer Publishing. (B) The same data as in (A) but plotted as a function of the Chol/PL mixing ratio in the suspension of lens lipid membranes. Notice that above the Chol/PL mixing ratio of ~2, the Chol crystals are formed in liposome suspensions. Thus, the Chol/PL molar ratio in PCDs and the amount of Chol forming CBDs should not increase further.

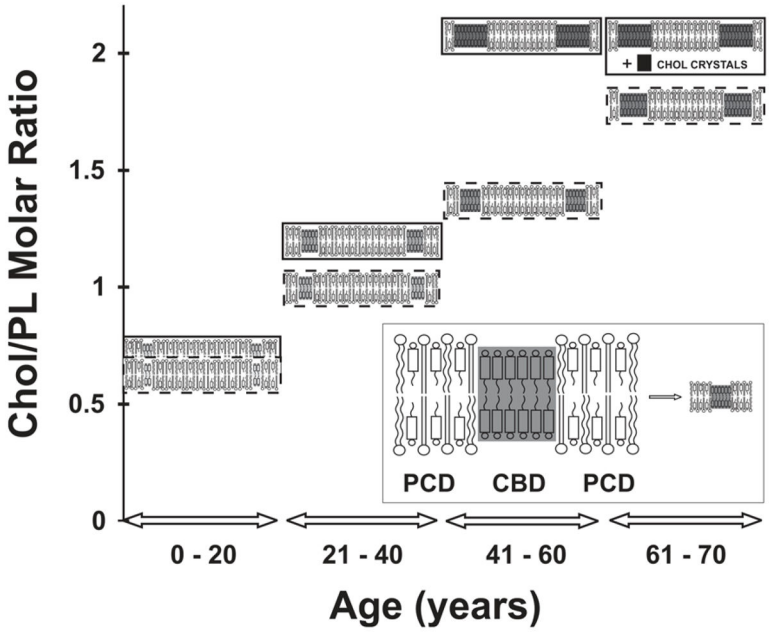

Figure 8.

Schematic drawing presenting changes in the organization of cortical (inside broken rectangle) and nuclear lens lipid membranes (inside solid rectangle) as functions of age and Chol content in investigated membranes. Excess Chol (above the Chol solubility threshold at ~2) forms Chol crystals, presumably outside the fiber cell membranes. Notice that with age and Chol content, the Chol/PL molar ratio in PCDs and the size of CBDs change. The shading of domains indicates changes in measured domains properties. Increased shading of CBDs indicates that measured properties (OTP (Fig. 6) and NIEDDA accessibility parameter (Fig. 7)) change from those similar to properties of the PCD. (Insert) An expanded drawing of the lens lipid membrane with indicated membrane domains.